Effective Model for Olefin/Paraffin Separation using (Co, Fe, Mn, Ni)-MOF-74

Luna-Triguero, A.; Vicent-Luna, J.M.; Becker, T.M.; Vlugt, T.J.H.; Dubbeldam, D.; Gómez-Álvarez, P.; Calero, S.

DOI
10.1002/slct.201601095

Publication date
2017

Document Version
Final published version

Published in
ChemistrySelect

ChemPubSoc Europe

DOI: 10.1002/slct.201601095

Chemistry SELECT Full Papers

Materials Science inc. Nanomaterials & Polymers

Effective Model for Olefin/Paraffin Separation using (Co, Fe, Mn, Ni)-MOF-74

Azahara Luna-Triguero,[a] Jose Manuel Vicent-Luna,[a] Tim M. Becker,[b] Thijs J. H. Vlugt,[b] David Dubbeldam,[c] Paula Gómez-Álvarez,*[a] and Sofia Calero*[a]

An increase in demand for energy efficient processes for the separation of saturated and unsaturated light hydrocarbons mixtures drives the need of noncryogenic processes. The adsorptive separation using Metal-Organic Frameworks with coordinatively unsaturated metal sites may provide a cost-effective alternative due to the strong binding of the metal cation with the unsaturated hydrocarbons. Since experiments on adsorption equilibrium of gas mixtures are challenging, we propose classical force field based simulations to analyse the ability of MOF-74 with different metal substitutions for the separation of C2 and C3 olefin/paraffin binary mixtures. We parametrized the force field by fitting to available experimental single-component adsorption isotherms of ethane, ethene, propane, and propene in M–MOF-74 (M=Co, Fe, Mn, and Ni). The force field was validated for a variety of temperatures ranged from 273 K to 353 K. We then conducted Monte Carlo simulations in the Grand-Canonical ensemble to elucidate the adsorption mechanisms of the saturated/unsaturated hydrocarbon mixtures, at 318 K and 353 K. We computed the adsorption isotherms, and from these the adsorption selectivity, and addressed the variations of MOF properties with different metal cations. Fe-based MOF-74 appears the best option for both ethane/ethene and propane/propene separation applications. This finding partly agrees with previous work based on the Ideal Adsorbed Solution Theory.

Introduction

Hydrocarbons with carbon numbers in the 1–3 range, namely methane, ethylene, ethane, propylene, and propane are very important energy resources and raw chemicals. The separation of light hydrocarbon mixtures is hence of great importance in the petrochemical and energy sectors, but it is challenging to perform this separation at the industrial scale.[1] Currently, the most commonly employed method is cryogenic distillation, which is based on the difference in the boiling points of the constituents.[2] This technology is however very energy-intensive due to the requirement of low temperatures and high pressures.[1] Thus, replacing large-scale cryogenic distillation with higher-temperature separation processes could potentially save energy consumption and reduce operating expenses. Among several new energy-efficient alternatives, adsorptive separation is one of the most promising.[3] While cryogenic distillation relies on small differences in the boiling points of olefin and paraffin components, adsorptive separations take advantage of other dissimilar physical properties, namely the kinetic diameter, polarity or polarizability of guest molecule. In this regard, the selection of a proper adsorbent with adequate selectivity and capacity is an important step in designing the adsorption process. The adsorptive separation of methane from C2 and C3 hydrocarbons is relatively easier since CH_4 is the smallest and least polarizable molecule, and hence it has weaker interactions within the pores.[4–6] However, separation of C2 and C3 olefin/paraffin mixtures is very difficult because these individual pair molecules have comparable sizes.

Metal-Organic Frameworks (MOFs) are porous materials that are receiving considerable attention for adsorptive gas separation applications.[7] They are crystalline organic-inorganic hybrid compounds formed by coordination of metal ions or clusters with organic linkers (bivalent or trivalent aromatic carboxylic acids or azoles) to form robust porous periodic frameworks. MOFs are well-known for their extremely high porosity, large surface areas, controllable pore structures, and versatile chemical compositions.[8] MOFs with coordinatively unsaturated metal clusters, which may be created by evacuation of frameworks that have metal-bound solvent molecules, have emerged as promising candidates to separate mixtures of saturated/unsaturated hydrocarbons at high temperatures,[9,10] dispensing with the need for cryogenic cooling. The unsaturated coordination sites at the metal center within the bulk of the material (also referred to as open metal sites, OMS) allow for the preferential adsorption of one hydrocarbon over the

[a] A. Luna-Triguero, J. M. Vicent-Luna, Dr. P. Gómez-Álvarez, Prof. S. Calero
Department of Physical, Chemical and Natural Systems
Universidad Pablo de Olavide
Ctra. Utrera km 1. ES-41013, Seville, Spain
E-mail: pgomalv1@upo.es
scalero@upo.es
[b] T. M. Becker, Prof. T. J. H. Vlugt
Engineering Thermodynamics, Process & Energy Department
Faculty of Mechanical, Maritime and Materials Engineering
Delft University of Technology
Leeghwaterstraat 39, 2628CB Delft, The Netherlands
[c] Dr. D. Dubbeldam
Van't Hoff Institute for Molecular Sciences
University of Amsterdam
Science Park 904, 1098 XH, Amsterdam, The Netherlands

Supporting information for this article is available on the WWW under http://dx.doi.org/10.1002/slct.201601095

other based on the difference in their electronic properties. Specifically, the OMS in the framework bind stronger olefins over paraffins. Several reports[11–15] have recently demonstrated the potential use of M_2(dobdc) compounds (M=Zn, Mn, Fe, Co, Ni; dobdc^{4-} = 2,5-dioxido-1,4-benzenedicarboxylate) for the separation of light hydrocarbons, as well as for other gas separations.[16–18] The members of M_2(dobdc) series are likewise referred to as M–MOF-74 and CPO-27-M. Zn-MOF-74 was first reported in 2005,[19] and isostructural systems with other metal centres have been subsequently presented.[20–23] The M–MOF-74 structures share the same network topology (bnn), infinite-rod secondary building unit (SBU) coordination scheme, 1-periodic hexagonal pore channel, and dobcd^{4-} linkers. Their crystal structures reveal nearly identical pore dimensions of approximately 12 Å. Available literature on olefin/paraffin separation in M–MOF-74 series is however based on results of the single-component adsorption performance.[11–13] Because of the difficulty of measuring adsorption equilibrium data of gas mixtures, the selectivity of the binary mixtures has been only theoretically estimated to date by using the Ideal Adsorbed Solution Theory (IAST) of Myers and Prausnitz from pure-component adsorption isotherms.[24] The molecular simulation technique represents a useful tool, but standard force fields often fail in describing adsorption at OMS,[25,26] probably attributed to interactions with the double bond of alkenes. Additionally, molecular simulations on adsorption equilibrium of mixtures entail high computational cost. With this in mind, the aim of our work is twofold: First, to parametrize the force field for these systems, and then, use molecular simulations to predict the separation process of the binary mixtures. More specifically, we parametrized the cross guest-host Lennard-Jones interaction for ethane, ethene, propane, and propene in M–MOF-74 series (M= Co, Fe, Mn, and Ni) by fitting to experimental data in the literature on pure-component adsorption equilibrium. The force field parameters were validated by comparing with experiments at different temperatures. This allowed us the computation of the adsorption isotherms of the saturated/unsaturated binary mixtures. For these adsorption calculations, we conduct Grand-Canonical Monte Carlo (GCMC) simulations at 318 K and 353 K, in order to observe the effect of the temperature, up to pressures of 100 bar. To evaluate whether a material is adsorption-selective for a particular task, the calculation of selectivity is extremely valuable. We evaluate changes in the adsorption properties of the MOF with variation of only the framework metal cation, and the efficiency of each material in terms of the adsorption selectivity.

The paper is organized as follows. Details of the simulations are described in *Methods*. The first part of *Results* section is devoted to force field parametrization and validation. Then, we report and analyze the adsorption performance of the saturated/unsaturated C2 and C3 binary mixtures in the various MOFs. In the *Conclusions* our main results are briefly summarized.

Results and Discussion

Pure–component adsorption isotherms: Force field parametrization and validation.

As it is exposed in *Methods*, the L–J parameters for framework atoms were taken from DREIDING[27] except those for metallic atoms, which correspond to UFF[28]. For describing the alkanes and alkenes, we used the models reported by Dubbeldam *et al.*[29,30] and Liu *et al.*[31], respectively. For these descriptions of the framework atoms and hydrocarbon guest molecules, Table 1 shows the proposed cross guest-host interaction parametrization. We obtained this force field by fitting to experimental data on pure-component equilibrium adsorption isotherms for ethane, ethene, propane, propene, as shown in the following figures. Specifically, the force field parameters were fitted to data at 318 K taken from Geier *et al.*[11] for all the metal sites except for Fe, which was taken from Bloch *et al.*[13]. Then, the force field was validated for Mn, Ni, Fe by comparing with data at 353 K taken from Geier *et al.*,[11] Mishra *et al.*,[14] and Bloch *et al.*,[13] respectively. In the case of Co, we compared with data from He *et al.*[12] at 273 K and 296 K, and from Geier *et al.*[11] and Mishra *et al.*[14] at 353 K. The set of starting fitting parameters were obtained by applying Lorentz-Berthelot (L–B) mixing rules and are listed in Table S1 of the Electronic Supporting Information (ESI). We mainly increased σ parameters, and slightly modified ε parameters characterizing cross interactions between adsorbate pseudo atoms and linker of the frameworks to obtain the shape of experimental isotherm. Then, we fit the metal-adsorbate parameters to reproduce accurately the isotherm for the different M–MOF-74 structures. With this procedure, the set of parameters for the adsorbate-organic linker interactions is the same for all the structures, and the proposed force field only differs on the specific adsorbate-metal parameters. It should be noted that M–MOF-74 structures are different, not only because they have different chemical composition, also the structure properties (i.e unit cell

Table 1. Lennard-Jones parameters characterizing cross interactions between hydrocarbon (saturated and unsaturated) and framework atoms developed in this work. ε_{ij}/k_B in K (top) and σ_{ij} in Å (bottom).

Atoms of the MOFs	Guest atoms			
	CH_3_sp3	CH_2_sp3	CH_2_sp2	CH_sp2
O	72.142	51.948	66.945	88.441
	3.532	3.566	3.967	3.285
C	71.895	51.770	66.716	88.138
	3.761	3.791	4.223	3.498
H	28.745	20.698	26.673	35.238
	3.435	3.471	3.854	3.194
Co	27.597	79.490	25.609	115.997
	3.317	3.325	3.684	3.149
Fe	34.555	114.842	98.664	148.965
	3.304	3.277	3.767	3.642
Mn	26.695	20.108	24.679	130.414
	3.359	3.365	3.731	3.667
Ni	28.567	20.570	26.509	35.020
	3.299	3.307	3.664	3.039

dimensions, surface area, pore volume, etc.) change slightly with the substitution of the metal.[11,32] With this in mind, the differences in the adsorption isotherm for the different M–MOF-74 could not be only related with the adsorbate-metal interactions. Also the interaction of the hydrocarbons with the environment near the metal should be considered and it is different for each structure. Moreover, hydrocarbons are modelled using a united atom description of the molecules which is developed for simplicity and transferability. Therefore the potential parameters for an isolated pseudo-atom and metal interaction cannot be related with the physical properties of the atoms.

Figure 1 shows experimental pure-component isotherms in a pressure range of 0–1000 kPa for the set of hydrocarbons

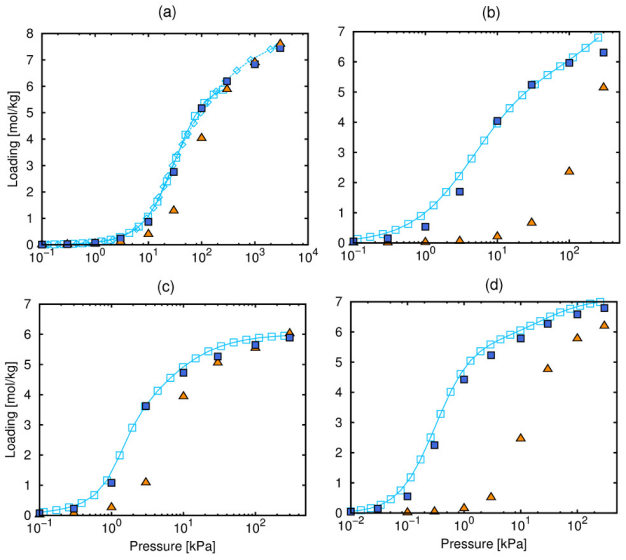

Figure 1. Pure-component adsorption isotherms of ethane (a), ethene (b), propane (c), and propene (d) in Co–MOF-74 at 318 K: Experiments[11] (open squares), computational data using standard Lorentz-Berthelot mixing rules (triangles), and using the proposed guest-host force field parametrization (closed squares).

along with computational results from using both standard L–B mixing rules (Table S1) and the proposed cross L–J parametrization (Table 1) at 318 K for the specific case of Co–MOF-74. As can be seen, simulations using L–B mixing rules produce larger onset pressures of adsorption, especially in the case of unsaturated hydrocarbons, and uptakes that are lower than experiments. This disagreement, found also in the literature,[33,34] clearly reveals the need of an appropriate force field for these systems. The force field parameters developed here allow the satisfactory experimental reproduction of the single-component isotherms of both alkanes and alkenes in Co–MOF-74. This can be extended for the rest of metal cations as shown in Figures S1-S3 of the ESI.

The suitability of the set of L–J parameters obtained by fitting to adsorption measurements of Figure 1 at 318 K has been explored at other temperatures for which experimental data are available. Figures 2 and 3 show the computed and experimental pure-component adsorption isotherms for the

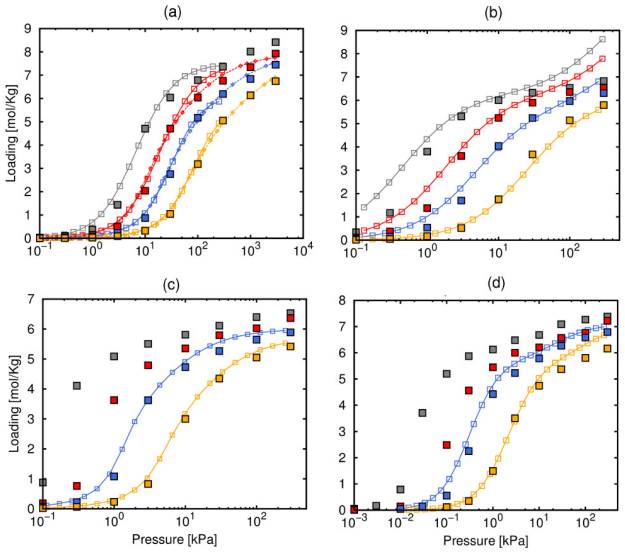

Figure 2. Pure-component adsorption isotherms of ethane (a), ethene (b), propane (c) and propene (d) in Co–MOF-74 at 273 K (grey), 296 K (red), 318 K (blue), 353 K (yellow): Experiments (open symbols)[11,12,14] computational using the proposed guest-host force field parametrization (closed symbols).

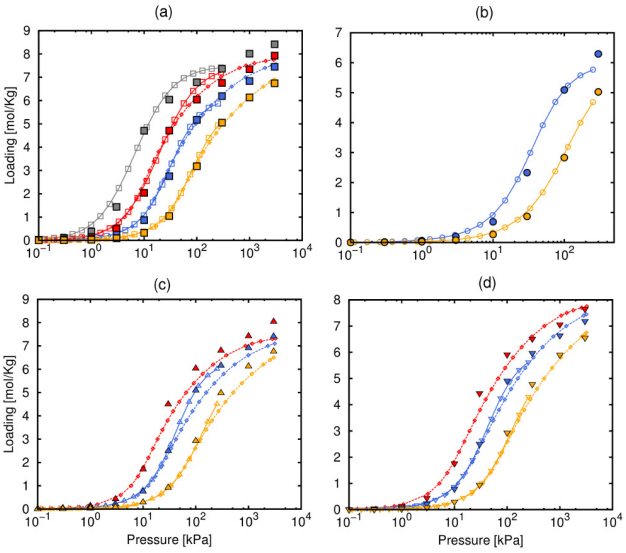

Figure 3. Pure-component adsorption isotherms of ethane in Co–MOF-74 (a), Fe-MOF-74 (b), Mn–MOF-74 (c), and Ni-MOF-74 (d) at 273 K (grey), 296 K (red), 318 K (blue), 353 K (yellow): Experiments (open symbols),[11–14] computational using the proposed guest-host force field parametrization (closed symbols).

various adsorbates in Co–MOF-74 and for ethane in the four members of the M–MOF-74 series (M=Co, Fe, Mn, and Ni), respectively, at temperatures ranging from 273 K to 353 K. As temperature increases, the onset pressures increase and the hydrocarbon uptakes decrease. We found our data to match

with measurements with relatively high accuracy for all considered adsorbates (Figure 2) and adsorbents (Figure 3). This agreement with experiments for the variety of temperatures points to the reliability and validation of the force field parametrization. Similar plots involving the remaining adsorbents and adsorbates are collected in Figures S4-S9 of the ESI, and also lead to such conclusion. Taking into account that we based on force fields describing C_n alkanes and alkenes, namely Dubbeldam *et al.*[29,30] and Liu *et al.*[31] respectively, this analysis could be extended to larger hydrocarbons, as it was previously shown for zeolites.[29–31] However, we cannot guarantee this due to the absence of experimental data.

To compare the behavior of adsorbates and adsorbents, Figure 4 shows the pure-component adsorption isotherms for

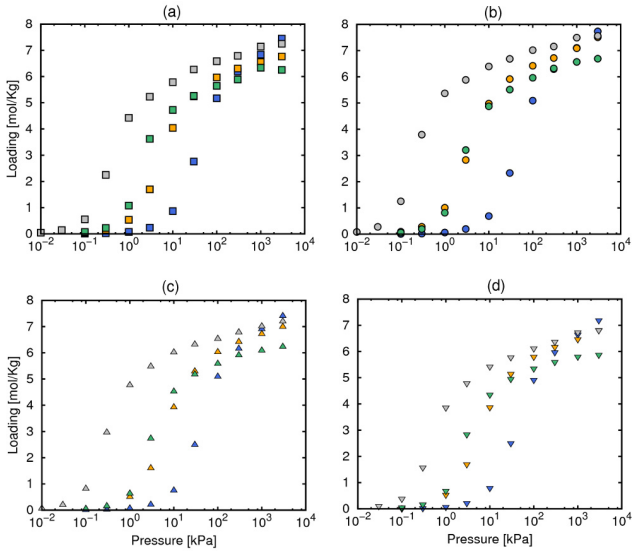

Figure 4. Computed pure-component adsorption isotherms of ethane (blue), ethene (yellow), propane (green) propene (grey) in Co–MOF-74 (a), Fe-MOF-74 (b), Mn–MOF-74 (c), and Ni-MOF-74 (d) at 318 K.

all guest molecules in each MOF at 318 K. Regardless of the metal, the onset pressures of adsorption follow the trend ethane > ethene > propane > propene. This is due to the increasing molecular size of the gas molecule, but also to the interaction of the exposed metal cations with the olefin π bond. While polarizability is an important factor in unsaturated hydrocarbon adsorption, the electron donating and accepting properties of the metal center must also be considered. Specifically, the framework metals that are more capable of accepting π electron density and/or donating electron density into the empty π orbital of the olefin are expected to show a stronger interaction. The reproduction of the experimental adsorption isotherms is an indication that proper adjustment of vdW terms seems to mimic the π-bonding in an approximate way. This is due to the proposed model could describe properly the entropic effects that govern the adsorption process as they depends mostly on the available space to a molecule and this is less sensitive to the potential energy surface. It is worth noting however the approximate character of the parametrization approach of this work, in the sense that QM calculations would be necessary for a precise description of the metal-hydrocarbon interactions[35–40] describing accurately the potential energy surface. But this is out of the scope of this work. Also, the uptake of the hydrocarbons in the low-coverage and intermediate regimes follows such (opposite) trend: ethane < ethene < propane <propene. At the highest values of pressure, packing effects play a role and the largest uptake corresponds to ethane. However, for C3 hydrocarbons, the amount of unsaturated hydrocarbon adsorbed is larger than the amount of saturated hydrocarbon over the entire pressure range in all the MOFs. The adsorption loadings vary between 6 and 8 mol·kg^{-1} depending on the adsorbate and, in a less extent, on the adsorbent. We reported energetic factors in Figure 5, where we depict the average guest-host potential

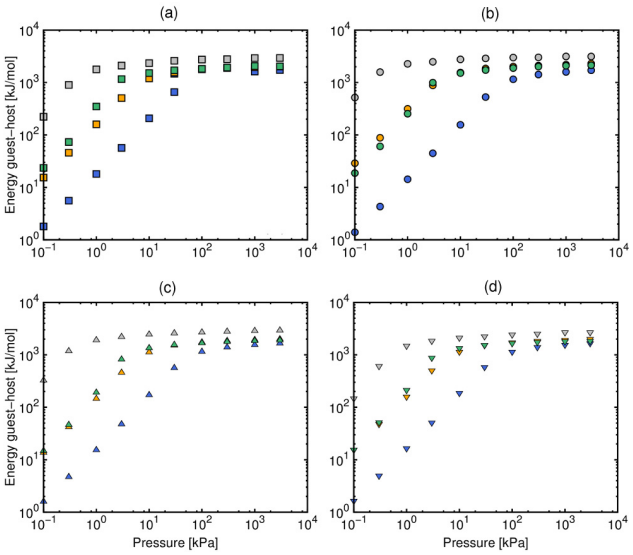

Figure 5. Average guest-host potential energy per mol of adsorbed guest molecules of pure ethane (blue), ethene (yellow), propane (green) and propene (grey) in in Co–MOF-74 (a), Fe-MOF-74 (b), Mn–MOF-74 (c), and Ni-MOF-74 (d) at 318 K.

energy per mol of adsorbed guest molecules as a function of fugacity for each system. The variation of the identity of the metal leads to considerable variations in the binding energies, which are closely related to the isotherms in Figure 4. This suggests that the strong interactions of adsorbates with the open metal sites govern the adsorption processes. The trends of both curves are however qualitatively distinctive at the highest pressures (and so uptakes) due to the significant guest-guest interactions. In the light of these results, a high adsorption selectivity for the unsaturated over saturated hydrocarbons is expected in the binary mixture adsorption.

Olefin/paraffin binary mixtures: adsorption isotherms and selectivity.

Since adsorption isotherms of gas mixtures cannot be conveniently and rapidly measured, its behavior has been predicted to date using adsorption models such as IAST[41] from experimental pure-component isotherms. Here we use the validated force field parameters of Table 1 to estimate the competitive adsorption of the saturated and unsaturated hydrocarbons. Figures 6 and 7 show the adsorption isotherms of the

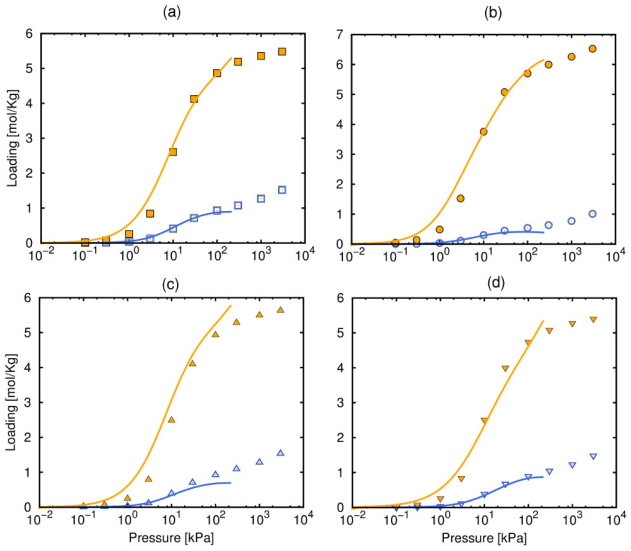

Figure 6. Computed adsorption isotherms of the equimolar binary ethane/ethene mixture in Co–MOF-74 (a), Fe-MOF-74 (b), Mn–MOF-74 (c), and Ni-MOF-74 (d) at 318 K from our MC simulations (points) and using IAST (lines) from theoretical fittings of pure-component isotherms reported in Geier *et al.*[11].

equimolar olefin/paraffin mixtures for C2 and C3, respectively, at 318 K and pressures up to 100 bar for the M–MOF-74 members, together with IAST calculations from data reported in Geier *et al.*[11] The much higher adsorption affinity to alkenes over alkanes is evident from both methods, IAST using the theoretical fittings for pure-component isotherms reported by Geier *et al.* and simulated isotherms for binary mixtures, which exhibit good agreement, especially at low pressures and for C2 hydrocarbons. As can be seen, this preferential alkene adsorption by the strong complexation between metal ions and the π orbital is more noticeable for C3 hydrocarbons. The adsorption of propane from the mixture is less than 1 mol·kg^{-1} regardless of the MOF. Generally speaking, for the purpose of comparing different materials and a rational choice of adsorbent for mixture separation, both high adsorption capacities and selectivities are desirable. In regards the former property, MOF-74 members further overcomes other candidate materials with limited uptake capacities, such as most zeolites. As it is apparent from these figures, although rather slightly larger for Fe-MOF-74, the capacity of the considered M–MOF-74 members is similar. The 12 Å-wide channels of these materials

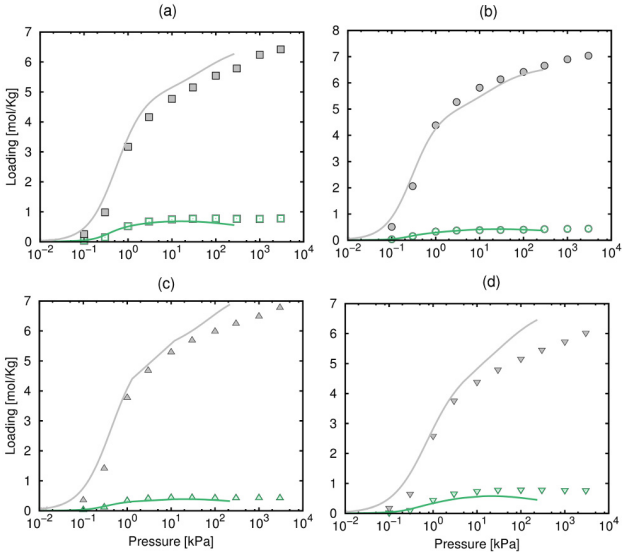

Figure 7. Computed adsorption isotherms of the equimolar binary propane/propene mixture in Co–MOF-74 (a), Fe-MOF-74 (b), Mn–MOF-74 (c), and Ni-MOF-74 (d) at 318 K from our MC simulations (points) and using IAST (lines) from theoretical fittings of pure-component isotherms reported in Geier *et al.*[11].

lead to large pore volumes and consequently high adsorption capacities. Besides, Fe-MOF-74 seems to be likewise the most selective, as well as Mn–MOF-74 in the case of C3 hydrocarbons. We next comprehensively evaluate the adsorption selectivity.

From the adsorption isotherms of the equimolar mixtures in Figures 6 and 7, we calculated the selectivity of alkenes over alkanes in each MOF-74 throughout the fugacity range in order to evaluate the efficacy of these materials for the proposed separations as well as the optimal pressure conditions. The obtained adsorption selectivities as a function of fugacity are shown in Figure 8. As can be seen, Fe-MOF-74 has the highest selectivity for separating both ethane/ethylene and propane/propylene pairs, in consistency with literature,[11,12] but Mn–MOF-74 shows also high selectivity ($>$ 10) for the latter pair. Particularly, the performance of Mn–MOF-74 is comparable to that of Fe-MOF-74 at the highest pressures. The Co and Ni analogues exhibit the lowest and similar selectivities for both separations, which is likely due to the weaker interactions between these metal cations and the unsaturated hydrocarbons. While the equilibrium selectivity of Fe-MOF-74 is maximum at low pressures and follows a clearly decreasing trend with fugacity for C2 hydrocarbons, it slightly varies with fugacity and reaches its highest values at atmospheric pressure for C3 hydrocarbons, which represents the lowest-operational costs. Since the exact composition of the olefin-paraffin mixture may vary significantly depending on the application, we conduct additional calculations throughout the concentration range. In Figure 9, we plot the adsorption loading of alkane/alkene mixtures for C2 and C3 hydrocarbons in Co–MOF-74 at 318 K and atmospheric pressure as a function of the respective alkane mole fractions in the bulk phase. The uptake of the

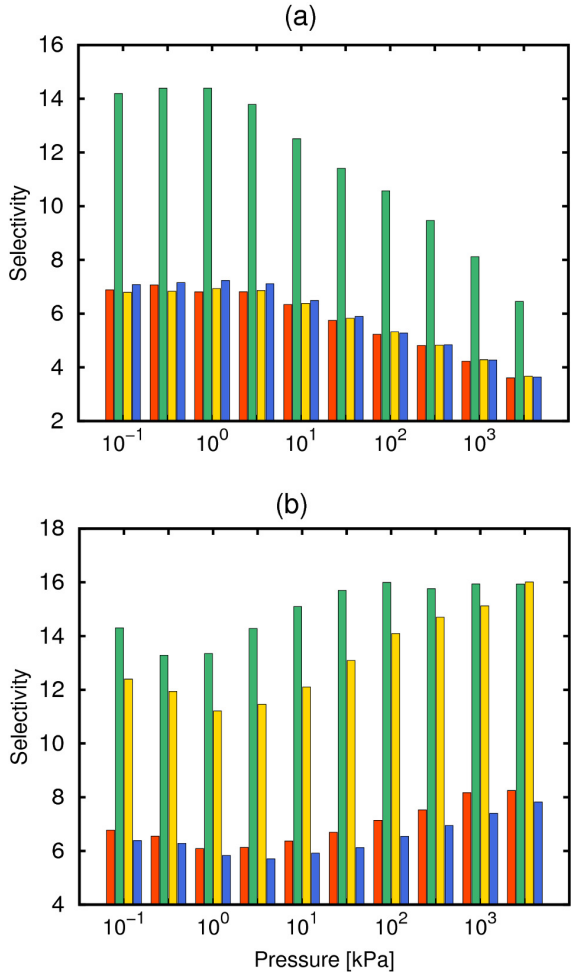

Figure 8. Adsorption selectivity of the equimolar ethane/ethene (a) and propane/propene (b) binary mixtures as a function of fugacity in Co–MOF-74 (red), Fe-MOF-74 (green), Mn–MOF-74 (yellow), and Ni-MOF-74 (blue) at 318 K.

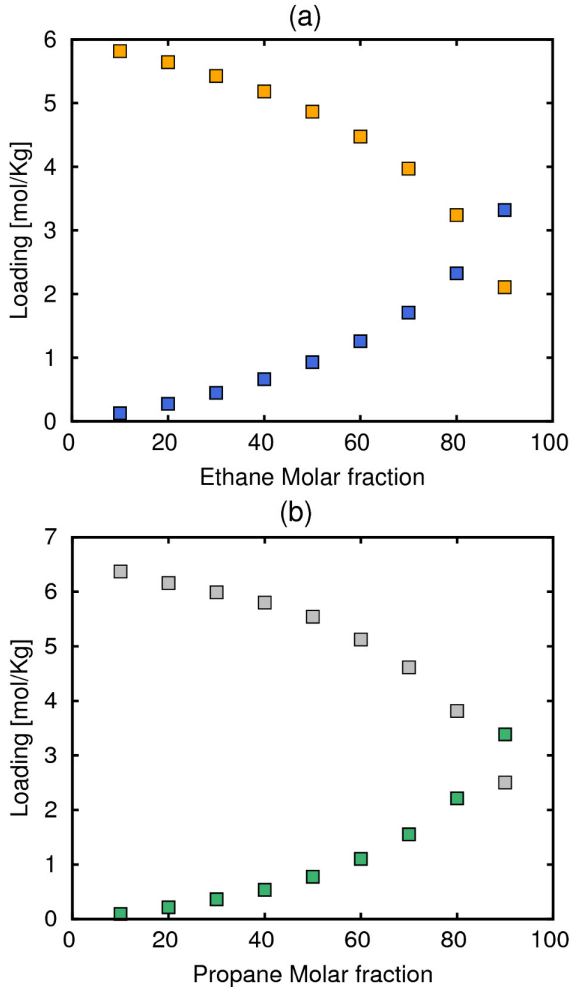

Figure 9. Adsorption loading of ethane (blue)/ethene (yellow), and propane (green)/propene (grey) in Co–MOF-74 at 318 K and 1 bar as a function of the alkane concentrations in the bulk phase for the respective binary mixtures.

unsaturated hydrocarbons is larger than for saturated except for high concentrations of the alkane in the bulk phase (above 90% approximately). Results for the remaining MOFs are qualitatively the same and provided in the ESI. Figure 10 shows our results of selectivity of alkenes over their alkane analogues as a function of the mixture composition in each MOF-74, together with IAST selectivity calculations for the same thermodynamic conditions (318 K, 1 bar) taken from Geier *et al.*[11] The selectivity values obtained by IAST are of the same order than ours but not coincident, and qualitative inconsistencies are also evident. Our values reveal that ethane/ethane selectivity slightly increases with increasing alkane concentration whereas it is unchanged or even decreases in the case of C3 hydrocarbons. The opposite trend is observed when using the IAST theory from pure-component adsorption data. Similarly to that occurring along the pressure range for equimolar mixtures, we identify Fe-MOF-74 as the best option for both saturated/unsaturated separations at any mixture contents, especially for ethane/ethylene. The selectivity of Mn–MOF-74 is also significant for C3 hydrocarbons. Geier *et al.*[11] found that Fe-MOF-74 and Mn–MOF-74 exhibit the highest selectivities for the separation of ethylene-ethane and propylene-propane mixtures, respectively. Nevertheless, it is worth noting that these considerable differences in the selectivity, and thus in the choice of the optimal candidates, between both methods actually arise from slight variations in the hydrocarbon loadings, as it is apparent from Figures 6 and 7 for the equimolar mixture. Since the selectivity entails the ratio of the uptakes of the mixture compounds, it is very sensitive to such values, especially for low values (below 1) as it is the case of alkanes.

According to the reported results at 318 K, we can state that the energy costs associated with large-scale industrial separation of light hydrocarbons by cryogenic distillation could be hence potentially lowered using these solid adsorbents (mainly Fe-MOF-74 and also Mn–MOF-74 for propane/propene) which operate at high temperatures. From a qualitative viewpoint, our simulations at 353 K reveal almost the same behavior on the adsorption selectivity for these binary mixtures in the

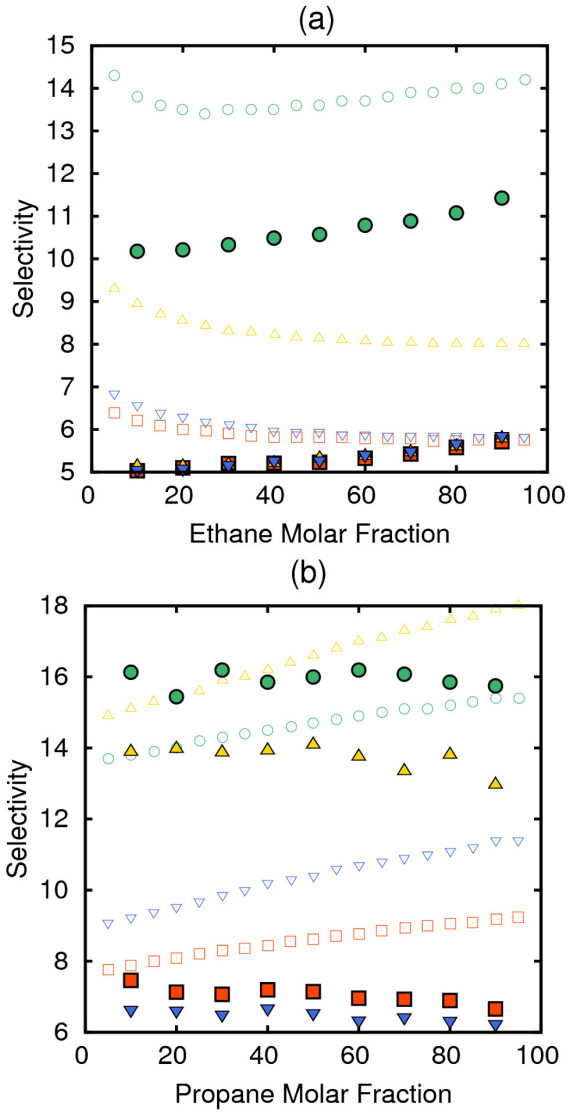

Figure 10. Adsorption selectivity of ethane/ethene (a) and propane/propene (b) binary mixtures as a function of the alkane concentrations in the bulk phase in Co–MOF-74 (red), Fe-MOF-74 (green), Mn–MOF-74 (yellow), and Ni-MOF-74 (blue) at 318 K and 1 bar together with results reported by Geier *et al.*[11] using IAST theory (open symbols with the same colour code).

MOF-74 members as that reported for 318 K throughout either the pressure or the composition range. This is evident from Figures S13 and S14 of the ESI. The selectivity values are however considerably reduced at such operating temperature.

As a downside, as reveal results of heats of adsorption for alkenes in Figure S15 of the ESI, the force field is not developed for precise energetic interactions that one molecule feels. It is developed for adsorption at finite loading and temperature. The model is therefore not straightforwardly transferable to other systems, and limited to the MOF-74 topology. MOF-74 is however a very challenging system by itself and the force field does allow to predict selectivities of mixtures, which is very hard to address experimentally. Besides, our results show that we do not need an accurate description of the QM-level interaction with the metal, but that, at finite temperature and loading, it can be effectively included in the adjusted Lennard-Jones interactions.

Conclusions

We studied the feasibility of M–MOF-74 (M=Co, Fe, Ni, Mn) series for olefin/paraffin separation by GCMC molecular simulations. Our computational results on pure-component adsorption match the experimental gas adsorption data for ethane, ethene, propane and propene, suggesting that the proposed force field parameters adequately capture the metal-guest interactions. These cross interactions are likely transferable to larger hydrocarbons. Using these sets of LJ parameters, simulations on the C2 and C3 saturated/unsaturated binary mixtures have been reported for the first time. The open metal sites in coordinatively unsaturated MOFs play a fundamental role to differentiate their interactions with the light hydrocarbons. The adsorption capacities are almost the same for all considered adsorbents, but the adsorption selectivity varies considerably. We found unsaturated hydrocarbons to be selectively retained by each considered material, but Fe-MOF-74 appears by far the best candidate for ethane/ethene separation applications. The adsorption selectivity of the Fe-based material is also the highest in the case of C3 hydrocarbon mixtures, but the performance of Mn–MOF-74 is likewise outstanding. These findings are qualitatively kept throughout the pressure and the composition ranges. In regards to the temperature dependence, we found selectivity values to notably decrease with increasing temperature, but the described behavior is likewise unchanged. While the most selective behavior of Fe-MOF-74 for separations of equimolar alkane/alkene mixtures involving C2 hydrocarbons is observed at low pressures, the optimal performance for C3 hydrocarbons occurs at the lowest-cost operational conditions (atmospheric pressure). Interestingly, our results on selectivity at 1 bar and 318 K as a function of the mixture composition partially match previously reported IAST calculations at the same thermodynamic conditions. This is due to the sensitivity of this magnitude to slight changes in the component uptakes. Indeed, we showed for the adsorption isotherms of the equimolar mixtures the agreement through both methods.

Supporting Information

Methods and Models and their references, table of the starting parameters for the force field fitting, curves of the force field fitting on a adsorption equilibrium of ethane, ethane, propane, propene in M–MOF-74 for M=Fe, Mn, and Ni, comparison between available experimental and computational single-component adsorption isotherms, computational adsorption isotherms of the saturated/unsaturated binary mixtures as a function of the mixture composition for C2 and C3 hydrocarbons, adsorption selectivities and heats of adsorptions.

Acknowledgements

The research leading to these results has received funding from the European Research Council under the European Union's Seventh Framework Programme (FP7/2007-2013) / ERC grant agreement n° [279520], from the MINECO (CTQ2013-48396-P), and from the Andalucía Region (FQM-1851).

This work was sponsored by NWO Exacte Wetenschappen (Physical Sciences) for the use of supercomputer facilities with finantial support from the Nederlandse Organisatie voor wetenschappelijk Onderzoek (Netherlands Organisation for Scientific research, NWO). TJHV acknowledges NWO-CW for a VICI grant.

Conflict of Interest

The authors declare no conflict of interest.

Keywords: adsorption · hydrocarbon separation · molecular simulation · open-metal site

[1] M. M. J. A. Moulijn, A. van Diepen. Alan E. Comyns, *Chemical process technology,* John Wiley & Sons, Ltd., Chichester, United Kingdom, 2013.
[2] R. B. Eldridge, *Ind. Eng. Chem. Res.* **1993**, *32*, 2208–2212.
[3] J. Gascon, W. Blom, A. van Miltenburg, A. Ferreira, R. Berger, F. Kapteijn, *Microporous Mesoporous Mater.* **2008**, *115*, 585–593.
[4] R. W. Triebe, F. H. Tezel, K. C. Khulbe, *Gas Sep. Purif.* **1996**, *10*, 81–84.
[5] A. J. Brown, N. A. Brunelli, K. Eum, F. Rashidi, J. R. Johnson, W. J. Koros, C. W. Jones, S. Nair, *Science* **2014**, *345*, 72–75.
[6] Z. Tan, K. E. Gubbins, *J. Phys. Chem* **1992**, *96*, 845–854.
[7] A. R. Millward, O. M. Yaghi, *J. Am. Chem. Soc.* **2005**, *127*, 17998–17999.
[8] P. Silva, S. M. F. Vilela, J. P. C. Tome, F. A. A. Paz, *Chem. Soc. Rev.* **2015**, *44*, 6774–6803.
[9] A. F. P. Ferreira, J. C. Santos, M. G. Plaza, N. Lamia, J. M. Loureiro, A. E. Rodrigues, *Chem. Eng. J.* **2011**, *167*, 1–12.
[10] K. Li, D. H. Olson, J. Seidel, T. J. Emge, H. Gong, H. Zeng, J. Li, *J. Am. Chem. Soc.* **2009**, *131*, 10368–10369.
[11] S. J. Geier, J. A. Mason, E. D. Bloch, W. L. Queen, M. R. Hudson, C. M. Brown, J. R. Long, *Chem. Sci.* **2013**, *4*, 2054–2061.
[12] Y. He, R. Krishna, B. Chen, *Energy Environ. Sci.* **2012**, *5*, 9107–9120.
[13] E. D. Bloch, W. L. Queen, R. Krishna, J. M. Zadrozny, C. M. Brown, J. R. Long, *Science* **2012**, *335*, 1606–1610.
[14] P. Mishra, S. Edubilli, B. Mandal, S. Gumma, *J. Phys. Chem. C* **2014**, *118*, 6847–6855.
[15] P. Verma, X. F. Xu, D. G. Truhlar, *J. Phys. Chem. C* **2013**, *117*, 12648–12660.
[16] S. R. Caskey, A. G. Wong-Foy, A. J. Matzger, *J. Am. Chem. Soc.* **2008**, *130*, 10870–10871.
[17] J. A. Botas, G. Calleja, M. Sanchez-Sanchez, M. Gisela Orcajo, *Int. J. Hydrogen Energy* **2011**, *36*, 10834–10844.
[18] M. H. Rosnes, M. Opitz, M. Frontzek, W. Lohstroh, J. P. Embs, P. A. Georgiev, P. D. C. Dietzel, *J. Mater. Chem A* **2015**, *3*, 4827–4839.
[19] N. L. Rosi, J. Kim, M. Eddaoudi, B. Chen, M. O'Keeffe, O. M. Yaghi, *J. Am. Chem. Soc.* **2005**, *127*, 1504–1518.
[20] P. D. Dietzel, Y. Morita, R. Blom, H. Fjellvåg, *Angew. Chem.* **2005**, *117*, 6512–6516.
[21] W. Zhou, H. Wu, T. Yildirim, *J. Am. Chem. Soc.* **2008**, *130*, 15268–15269.
[22] S. Bhattacharjee, J.-S. Choi, S.-T. Yang, S. B. Choi, J. Kim, W.-S. Ahn, *J. Nanosci. Nanotechnol.* **2010**, *10*, 135–141.
[23] P. D. C. Dietzel, B. Panella, M. Hirscher, R. Blom, H. Fjellvag, *Chem. Commun.* **2006**, 959–961.
[24] A. Myers, J. M. Prausnitz, *AIChE J.* **1965**, *11*, 121–127.
[25] C. Chmelik, J. Kaerger, M. Wiebcke, J. Caro, J. M. van Baten, R. Krishna, *Microporous Mesoporous Mater.* **2009**, *117*, 22–32.
[26] P. G. M. Mileo, C. L. Cavalcante Jr., J. Moellmer, M. Lange, J. Hofmann, S. M. P. Lucena, *Colloids Surf., A* **2014**, *462*, 194–201.
[27] S. L. Mayo, B. D. Olafson, W. A. Goddard, *J. Phys. Chem* **1990**, *94*, 8897–8909.
[28] A. K. Rappe, C. J. Casewit, K. S. Colwell, W. A. Goddard, W. M. Skiff, *J. Am. Chem. Soc.* **1992**, *114*, 10024–10035.
[29] D. Dubbeldam, S. Calero, T. J. H. Vlugt, R. Krishna, T. L. M. Maesen, E. Beerdsen, B. Smit, *Phys. Rev. Lett.* **2004**, *93*, 088302–088302.
[30] D. Dubbeldam, S. Calero, T. J. H. Vlugt, R. Krishna, T. L. M. Maesen, B. Smit, *J. Phys. Chem. B* **2004**, *108*, 12301–12313.
[31] B. Liu, B. Smit, F. Rey, S. Valencia, S. Calero, *J. Phys. Chem. C* **2008**, *112*, 2492–2498.
[32] D. Yu, A. O. Yazaydin, J. R. Lane, P. D. C. Dietzel, R. Q. Snurr, *Chem. Sci.* **2013**, *4*, 3544–3556.
[33] Y.-S. Bae, C. Y. Lee, K. C. Kim, O. K. Farha, P. Nickias, J. T. Hupp, S. T. Nguyen, R. Q. Snurr, *Angew. Chem.* **2012**, *51*, 1857–1860.
[34] Z. Bao, S. Alnemrat, L. Yu, I. Vasiliev, Q. Ren, X. Lu, S. Deng, *Langmuir* **2011**, *27*, 13554–13562.
[35] A. N. Rudenko, S. Bendt, F. J. Keil, *J. Phys. Chem. C* **2014**, *118*, 16218–16227.
[36] P. Verma, X. Xu, D. G. Truhlar, *J. Phys. Chem. C* **2013**, *117*, 12648–12660.
[37] J. S. Lee, B. Vlaisavljevich, D. K. Britt, C. M. Brown, M. Haranczyk, J. B. Neaton, B. Smit, J. R. Long, W. L. Queen, *Adv. Mater.* **2015**, *27*, 5785–5796.
[38] K. Sillar, J. Sauer, *J. Am. Chem. Soc.* **2012**, *134*, 18354–18365.
[39] H. Kim, J. Park, Y. Jung, *Phys. Chem. Chem. Phys.* **2013**, *15*, 19644–19650.
[40] G. D. Degaga, L. Valenzano, *Chem. Phys. Lett.* **2016**, *660*, 313–319.
[41] S. R. G. Balestra, R. Bueno-Perez, S. Calero, *Zenodo* **2016.**

Submitted: August 8, 2016
Accepted: January 4, 2017